

Controlled Electrostatic Gating of Carbon Nanotube FET Devices

Alexander B. Artyukhin,^{†,‡} Michael Stadermann,[†] Raymond W. Friddle,[†]
Pieter Stroeve,[‡] Olgica Bakajin,[†] and Aleksandr Noy*,[†]

Chemistry and Materials Science Directorate, Lawrence Livermore National Laboratory, Livermore, California 94550, and Department of Chemical Engineering and Materials Science, University of California, Davis, California 95616

Received June 9, 2006

ABSTRACT

Carbon nanotube transistors are a promising platform for the next generation of nonoptical biosensors. However, the exact nature of the biomolecule interactions with nanotubes in these devices remains unknown, creating one of the major obstacles to their practical use. We assembled alternating layers of oppositely charged polyelectrolytes on the carbon nanotube transistors to mimic gating of these devices by charged molecules. The devices showed reproducible oscillations of the transistor threshold voltage depending on the polarity of the outer polymer layer in the multilayer film. This behavior shows excellent agreement with the predictions of a simple electrostatic model. Finally, we demonstrate that complex interactions of adsorbed species with the device substrate and the surrounding electrolyte can produce significant and sometimes unexpected effects on the device characteristics.

Use of semiconducting single-wall carbon nanotubes (SWNTs) for chemical and biological sensing relies on the extreme sensitivity of the nanotube electrical properties to local chemical environments. Direct electrical detection of label-free biomolecules with SWNT field-effect transistors (FETs) would have significant advantages over existing detection methods. Since the pioneering work by Dai¹ and colleagues, researchers have attempted to use carbon nanotubes to detect a variety of species, ranging from simple inorganic molecules^{2–6} to DNA⁷ and proteins.^{8–14} At the same time, an alternative platform based on silicon nanowire transistors has progressed significantly, demonstrating specific detection of single viruses¹⁵ and femtomolar concentrations of proteins in complex mixtures.¹⁶ The use of field-effect transistor devices to detect changes at the interface due to adsorption of charged species dates back to the early 1970s,¹⁷ and a number of experimental and theoretical works using conventional silicon-based VLSI transistor devices contributed to our understanding of the operation of these devices.^{18–24} Nevertheless, the nature of nanotube–molecule interactions and the mechanisms by which these interactions change the nanotube conductance remain largely unknown.¹¹

Rational design of carbon nanotube sensors requires understanding of the mechanisms responsible for signal generation. Biosensors usually operate at near-physiological conditions, so it is particularly important to understand the

interactions of charged biomolecules with nanotubes in aqueous ionic solutions. Adsorbates may change charge carrier density in a semiconducting SWNT using two possible mechanisms: capacitive gating or partial electron transfer, and both mechanisms can work simultaneously for real-world samples. The capacitive gating mechanism relies on altering the electrostatic field around the nanotube. Such gating happens when we apply voltage to the back of the Si substrate on which the nanotube device rests, or to the electrolyte surrounding the nanotube. In the latter case, the field is transmitted to the nanotube by ions that form an ionic double layer around the nanotube,²⁵ and it is easy to envision the same type of gating taking place when a charged analyte species approaches the nanotube. The second mechanism involves direct doping by partial electron transfer to or from the nanotube. This pathway is common for species with high redox potentials compared to the nanotube,^{3,26–29} although McEuen and colleagues questioned this mechanism recently.³⁰

In this work, we focused on the capacitive gating of carbon nanotubes, since it represents perhaps the most general gating mechanism, because most biomolecules bear at least some charge in aqueous solutions. Researchers often attribute changes in nanotube conductance upon addition of biomolecules to the impact that their charge has on the nanotube; yet sometimes conductance changes occur in the opposite direction from what we expect based on molecular charge.¹¹ It is also worth noting that most biosensing experiments with nanotube FETs so far have utilized nanotube channels pinned

* Corresponding author. E-mail: noy1@llnl.gov.

[†] Lawrence Livermore National Laboratory.

[‡] University of California Davis.

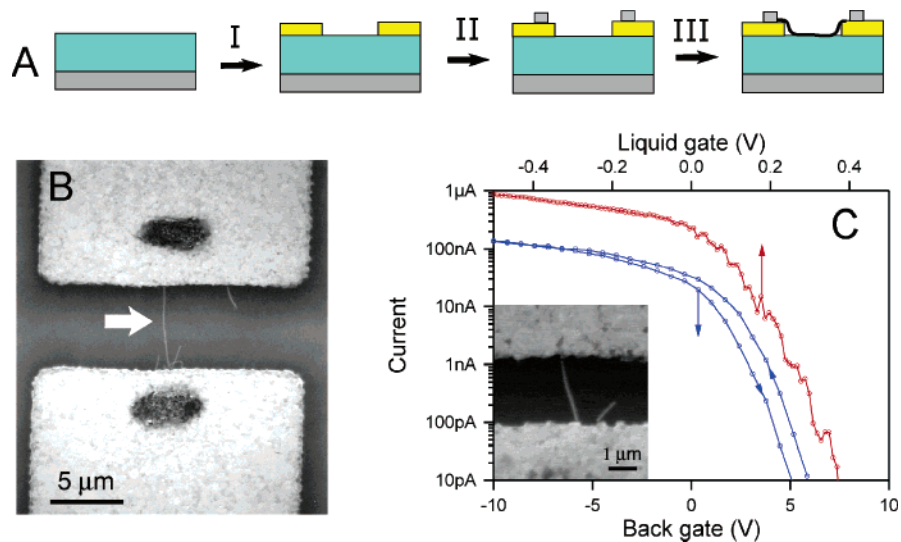


Figure 1. Fabrication and characterization of carbon nanotube devices. (A) Schematics of device fabrication: (I) patterning metal electrodes on SiO₂/Si wafer, (II) catalyst deposition, and (III) carbon nanotube growth by catalytic CVD. (B) SEM image of the final device, the arrow points to an SWNT bridging two electrodes. (C) Transfer characteristics of a representative SWNT device (measured using a source-drain voltage of 100 mV) in air (blue curve) and 100 mM NaCl in water (red curve). A SEM image of the device is shown in the inset.

to the substrate surface, typically SiO₂, and that this surface is negatively charged under physiological conditions.³¹ This charge, which is also sensitive to pH and ionic strength,³² will obviously contribute to the field acting on the carbon nanotube.³³ To study the effect of molecular electrostatic fields on the nanotube, we used layer-by-layer adsorption of highly charged polymers³⁴ onto SWNT FET devices. We also investigated how variations in SiO₂ surface potential induced by change in ionic strength influence nanotube FET performance. Finally, we showed that polymer adsorption may change the surface ionization of the substrate and that at certain conditions a combination of both effects is responsible for the seemingly unexpected shifts in the device characteristics.

Carbon Nanotube Transistor Fabrication. Our device fabrication sequence started with patterning electrodes (5 nm Cr, 50 nm Pt)³⁵ on top of a 2.5- μ m-thick layer of thermally grown oxide on a highly doped Si wafer (Figure 1a). We then lithographically patterned the catalyst islands (10 nm Al, 3 Å Mo, 5 Å Fe)^{36,37} on top of the electrodes. In the final step we grew SWCNTs from the catalyst islands using ethylene-based CVD growth.^{38–40} In this paper, we report only results obtained on devices that consist of individual SWNTs bridging the electrodes (Figure 1b). Our fabrication procedure produced high-quality devices: our transistors typically had on/off ratios of 10⁴ or greater; the subthreshold slope in water was close to the maximum theoretical value (ca. 70 mV/dec), and the devices achieved on-state conductance values close to 10 μ S (Figure 1c).

Electrical Measurements in Aqueous Solutions. For electrical characterization of our devices in liquid, we mounted the chip in a custom-made flow cell that incorporated an additional electrode, which allowed us to apply the gating voltage through the electrolyte solution.²⁵ The polyelectrolyte layers were deposited by passing a 50 mM solution of a polyelectrolyte [polyallylamine hydrochloride (PAH), sodium polystyrenesulfonate (PSS), or polydial-

lyldimethylammonium chloride (PDDA)] through the cell, starting with a polycation. No additional background electrolyte was present during polymer adsorption. After rinsing the cell with pure water to remove the excess polyelectrolyte, we filled it with the NaCl solution that we used for electrical characterization. For measurements in the dry state, we placed a drop of polymer solution on the chip for 30 min, then rinsed it with water, and dried it under a nitrogen stream. In this paper, we concentrate on the results obtained using PAH/PSS multilayers; PDDA/PSS multilayers produced qualitatively similar results.

Gating of CNT Transistors by Polyelectrolyte Multilayers. Sequential adsorption of polyelectrolytes on SWNT FETs shifts the transfer characteristics of the devices. After adsorption of the first layer, the I - V curve oscillates between two distinct states, depending on the sign of the outer polymer layer (Figure 2a). When the multilayer structure is terminated with the positively charged PAH layer, the curve shifts to more negative gate voltages, and when the film terminates with the negatively charged PSS layer, the curve shifts to positive gate voltage values. Qualitatively, this result is easy to understand. When a positively charged PAH layer is situated close to the nanotube, we need to apply more negative gate voltage to compensate for this charge. By the same token, a negatively charged PSS layer will require more positive gate voltage to compensate for the additional charge. Because of the reversal of the surface charge upon adsorption of each polymer layer,⁴¹ the periodic behavior should continue as we add more layers. Indeed, measured shifts of the threshold voltage confirm this trend (Figure 2b).

To demonstrate the electrostatic nature of the observed shifts, we have compared this data with the predictions of the model that Neff et al. initially developed to describe electrostatic contribution to the surface potential from polyelectrolyte multilayer buildup.⁴² This model describes the electrostatic potential shift at a surface covered with alternating layers of charged species and considers the

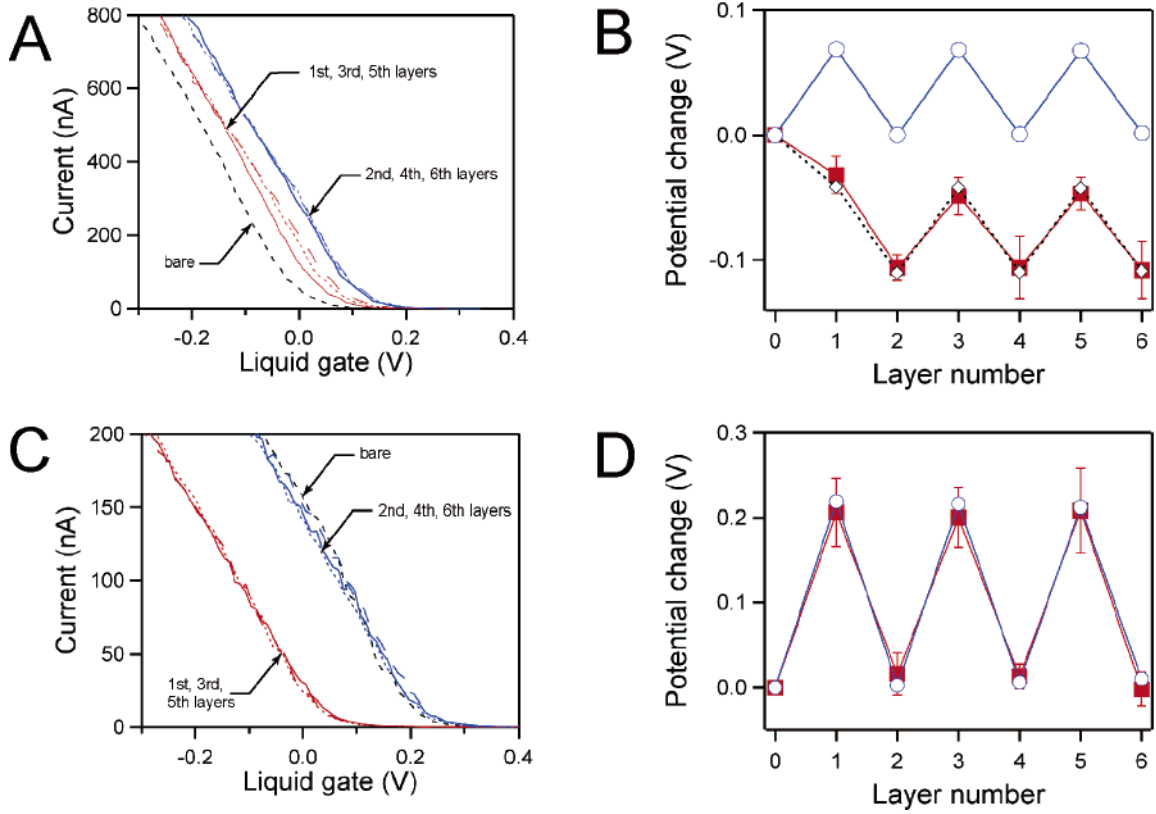


Figure 2. Transfer characteristics of carbon nanotube FET devices as a function of PAH/PSS multilayer adsorption in (A and B) 100 mM NaCl, and (C and D) 1 mM NaCl solutions. (A and C) Transfer characteristics of the device before (black short dash line) and after adsorption of polymer multilayers terminated with PAH (red lines) and PSS (blue lines). Solid lines, 1st and 2nd layers; dotted lines, 3rd and 4th layers; dashed lines, 5th and 6th layers. (B and D) Measured device threshold voltage shifts (red squares) and calculated surface potential changes (blue circles) as a function of number of adsorbed polymer layers. Threshold voltage of uncoated device and surface potential of bare SiO₂ surface served as reference points. Black diamonds and the dotted line in B represents the surface potential change calculated by taking into account the charge regulation at the surface.

contributions to the electrostatic potential from several sources: (1) ionized silicon oxide substrate surface, (2) polyelectrolyte multilayers, and (3) bulk electrolyte solution.⁴² In the general case where we apply a potential difference, U , between the nanotube and the gate electrode, the electrostatic potential at the surface, ψ_s , is

$$\psi_s(N) = \frac{U - \frac{1}{C_D}(-1)^N \frac{\sigma_p}{2}}{\frac{C_p}{C_D} \sinh(\kappa_p N d) + \cosh(\kappa_p N d)} \quad (1)$$

where $C_p = \kappa_p \epsilon_p \epsilon_0$ and $C_D = \kappa_w \epsilon_w \epsilon_0$ are the characteristic capacitances of polymer multilayer and bulk solution per area, κ_p and κ_w are the Debye lengths in polymer film and bulk solution, ϵ_p and ϵ_w are the dielectric constants of polymer film and bulk solution, ϵ_0 is the dielectric permittivity of vacuum, N is the number of polymer layers, d is the thickness of each layer, and σ_p is the surface charge density of polyelectrolyte layer. We chose σ_p to be twice the surface charge density of the silicon oxide substrate, σ_1 .^{41,43,44} Note that literature contains all of the parameter values for this model (Table 1); therefore, we can calculate the change in the electrostatic potential at SiO₂ interface with

Table 1. Parameter Values Used for Surface Potential Calculation upon Polyelectrolyte Layer-by-Layer Deposition

parameter	value
κ_p^{-1}	20 nm ⁵⁰
ϵ_p	30 ^{42,50,54}
d	1 nm ⁴¹
σ_1	-2.5 $\mu\text{C}/\text{cm}^2$ (100 mM NaCl), -0.8 $\mu\text{C}/\text{cm}^2$ (1 mM NaCl) ³²

no fitting parameters. The calculated shifts (blue trace in Figure 2b) follow the same periodic behavior that we observe in the experiment. More importantly, the calculated shifts match the measured shifts for adsorption of all layers except the first layer, which shifts the threshold voltage in the opposite direction from the calculated value. To explain this phenomenon, we need to consider the effect of the charged species on the ionization state of the SiO₂ surface.

The silanol groups on the surface of silicon oxide are weakly acidic, and the surface is negatively charged at pH values above 3. According to the Grahame equation,⁴⁵ varying the degree of dissociation and/or screening of surface charges will change the surface potential, ψ_s

$$\sigma = \sqrt{8\epsilon_0 k T n_0} \sinh\left(\frac{e\psi_s}{2kT}\right) \quad (2)$$

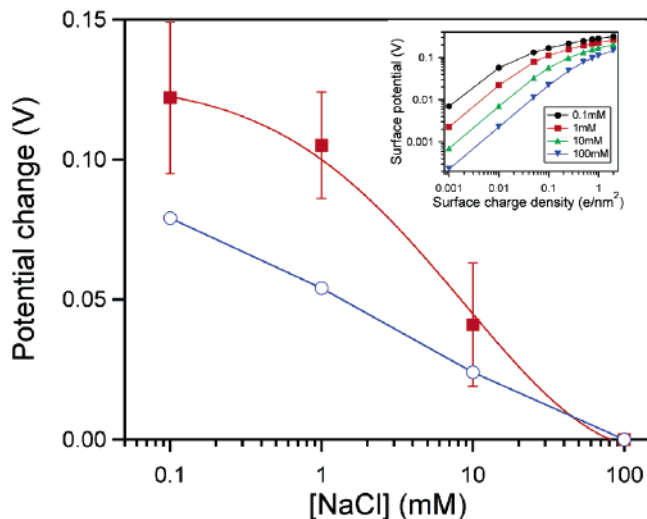


Figure 3. Measured device threshold voltage shift (red squares) compared to the calculated surface potential change (blue circles) as a function of NaCl concentration. Threshold voltage and surface potential at 100 mM NaCl served as reference points. Inset: surface potential at the silicon oxide surface as a function of surface charge density at different solution ionic strengths (calculated from the Grahame equation, eq 2).

where σ is the surface charge density, ϵ is the dielectric constant of the medium, k is the Boltzmann constant, n_0 is the bulk ion concentration, T is the temperature, and e is the electron charge. Lieber and co-workers used this effect with considerable success in their design of a silicon nanowire pH sensor;⁴⁶ yet for many sensing applications, variation in salt concentration, pH, or contamination can lead to unintended changes in surface ionization and thus complicate the device response. We have examined SWNT device characteristics in solutions of various ionic strengths and found that the nanotube source–drain current versus gate voltage curve shifted to more negative gate voltages upon increasing NaCl concentration (Figure 3).

Increase of ionic strength changes the SiO₂ surface by two competing processes. First, electrostatic screening reduces the surface potential (see eq 2 and Figure 3, inset). At the same time, efficient screening allows more silanol groups to ionize, causing an increase in surface charge density.³² When we combine these two opposite effects and substitute the literature value for the SiO₂ surface charge density³² into the Grahame equation, the absolute value of the surface potential decreases with increasing salt concentration (Figure 3, blue trace). As the surface potential becomes less negative, a more negative gate voltage is necessary to compensate for this change. Although this simple model predicts the direction of the nanotube threshold shift correctly, it underestimates the magnitude of the shift by about a factor of 2 (Figure 3). This discrepancy likely originates from the uncertainty in the value of the SiO₂ surface charge density. The surface charge density depends on the details of surface preparation, such as thermal treatment and hydration.³¹ Most of the literature values were measured on colloidal particles,^{32,47–49} whereas our substrate is a thermally grown oxide layer on a flat Si wafer. For consistency, we used the same surface charge density data that we used for modeling polyelectrolyte

adsorption (see Table 1), but we note that higher SiO₂ surface charge densities, such as those reported by Tadros,⁴⁹ produce a better fit to the data in Figure 3 (not shown).

Charge regulation at the interface plays a critical role in determining the device response to the adsorption of the first polymer layer. The observed shift in the “opposite” direction is also strikingly similar to effects that Dai and co-workers observed in protein sensing experiments.¹¹ In that case it was conceivable that, depending on the protein conformation on the surface, local fields of ionized residues may play a bigger role than the net charge of the molecule; however, this explanation is unlikely to apply for our experiments where we used a polymer with identically charged monomer units. Instead, we need to look at the changes in the local environment at the carbon nanotube. The concentration of mobile ions in polyelectrolyte multilayers is low and falls in the range of 0.1–1 mM for the PAH/PSS system used in our experiments.⁵⁰ Thus, even though we take measurements at the bulk salt concentrations of 100 mM (Figure 2a,b), the local ionic strength in the vicinity of the SiO₂ surface is reduced by 2 orders of magnitude (from 100 mM to about 1 mM) once the first polymer layer adsorbs. This drop in ionic strength would increase the negative surface potential by approximately 100 mV (Figure 3). We can estimate the pure polyelectrolyte contribution to the potential change at 100 mM NaCl in the bulk as 70 mV (Figure 2b). The combined effect from these two sources changes the potential by 30 mV in the *opposite* direction from what we expect based solely on the polymer charge. This number is in excellent agreement with the measured shift. Once the first polymer layer is adsorbed, the following layers will not change the ionic conditions near the silicon oxide surface; therefore, all subsequently adsorbed layers should generate shifts based purely on the electrostatic contributions. Indeed, if we incorporate this one-time shift due to the charge regulation in our model, the calculated potential change matches the experimental trend (Figure 2b, black diamonds).

This model also predicts that the anomalous shift upon addition of the first polymer layer should vanish when we perform measurements at low background electrolyte concentration. In this case, the local ionic strength in the vicinity of the SiO₂ substrate does not change upon adsorption of the first layer. Indeed, when we measured the response of the nanotube transistors to adsorption of PAH/PSS multilayers in 1 mM NaCl (Figure 2c), the anomalous shift upon addition of the first layer vanished and the measured shifts showed perfect agreement with the model prediction (Figure 2d). Note also that the magnitude of the SWNT threshold voltage shift upon polyelectrolyte adsorption increases as the ionic strength decreases (70 mV at 100 mM vs 200 mV at 1 mM) due to less efficient screening of polyelectrolyte charges at the polymer–solution interface.

Interestingly, SWNT devices also respond to polyelectrolyte multilayers in the dry state, showing qualitatively similar periodic threshold voltage oscillations (see the Supporting Information). In that case, however, the magnitude of the shift was approximately 20 times larger than the shifts recorded in 100 mM NaCl solution. The data also showed

more scatter in the dry state compared to measurements in solution. We attribute increased scattering to uncertainties in the residual water content in the multilayers that have a pronounced effect on ion mobility and dielectric properties of the film.^{50,51} This uncertainty is not surprising because polyelectrolyte films contain water even in the dry state;^{52,53} furthermore, polymers quickly absorb water from humid air after drying.⁵¹

Charge regulation at the interface can have important consequences for biological sensing in aqueous solutions. The magnitude of the threshold voltage shift upon adsorption of highly charged polyelectrolytes at close-to-physiological conditions (100 mM NaCl) is about 70 mV. For high-quality devices at optimized conditions, this value will produce current modulation of about an order of magnitude. Proteins have significantly lower charge density than polyelectrolytes and should therefore cause a considerably smaller change. If we assume that a protein molecule has a charge density that is 10 times lower than that of a strong polyelectrolyte, then we expect to see threshold shifts of only a few millivolts. This number is close to the values observed for DNA and protein detection experiments using silicon FETs and illustrates a general problem of low sensitivity for the field-effect-based sensing platform.^{18,24} Lowering the ionic strength of the solution results in a stronger response (compare Figure 2a and c). Researchers have observed similar effects in Si transistor devices previously and recognized low solution ionic strength as one of the prerequisites for sensitive field-effect detection. Changes in the surface properties of the substrate upon analyte adsorption or changes in the solution composition may complicate the matters even further. An interesting alternative to avoid the effects of surface charge regulation would be to use nonionizable substrate surfaces (or a chemical modification of the substrate), or to switch to using suspended nanotube devices that will not be sensitive to changes in the surface potential.

We have shown that sequential adsorption of positively and negatively charged polymers onto semiconducting SWNT devices produces regular oscillations of the device threshold voltage. The behavior is well described by a model taking into account the potential change at the nanotube due to the buildup of alternating oppositely charged layers. We also demonstrated that a change in surface ionization has significant impact on the device characteristics, as evidenced by the anomalous response to the deposition of the first polymer layer. Our results underscore the necessity of controlling substrate surfaces for the design of reliable and sensitive FET-based sensors.

Acknowledgment. A.B.A. and R.W.F. acknowledge an SEGR Fellowship from LLNL. M.S., O.B., and A.N. acknowledge support from the DARPA MGA program. This work was performed under the auspices of the U.S. Department of Energy by the University of California, Lawrence Livermore National Laboratory, under Contract No. W-7405-Eng-48.

Supporting Information Available: Figure S1. Comparison of measured and calculated device voltage threshold

shifts in dry state. This material is available free of charge via the Internet at <http://pubs.acs.org>.

References

- (1) Kong, J.; Franklin, N. R.; Zhou, C. W.; Chapline, M. G.; Peng, S.; Cho, K. J.; Dai, H. J. *Science* **2000**, *287*, 622.
- (2) Someya, T.; Small, J.; Kim, P.; Nuckolls, C.; Yardley, J. T. *Nano Lett.* **2003**, *3*, 877.
- (3) Bradley, K.; Gabriel, J. C. P.; Briman, M.; Star, A.; Gruner, G. *Phys. Rev. Lett.* **2003**, *91*, 218301.
- (4) Novak, J. P.; Snow, E. S.; Houser, E. J.; Park, D.; Stepnowski, J. L.; McGill, R. A. *Appl. Phys. Lett.* **2003**, *83*, 4026.
- (5) Kong, J.; Chapline, M. G.; Dai, H. J. *Adv. Mater.* **2001**, *13*, 1384.
- (6) Star, A.; Han, T. R.; Joshi, V.; Gabriel, J. C. P.; Gruner, G. *Adv. Mater.* **2004**, *16*, 2049.
- (7) Star, A.; Tu, E.; Niemann, J.; Gabriel, J. C. P.; Joiner, C. S.; Valcke, C. *Proc. Natl. Acad. Sci. U.S.A.* **2006**, *103*, 921.
- (8) Star, A.; Gabriel, J. C. P.; Bradley, K.; Gruner, G. *Nano Lett.* **2003**, *3*, 459.
- (9) Chen, R. J.; Choi, H. C.; Bangsaruntip, S.; Yenilmez, E.; Tang, X. W.; Wang, Q.; Chang, Y. L.; Dai, H. J. *J. Am. Chem. Soc.* **2004**, *126*, 1563.
- (10) Boussaad, S.; Tao, N. J.; Zhang, R.; Hopson, T.; Nagahara, L. A. *Chem. Commun.* **2003**, 1502.
- (11) Chen, R. J.; Bangsaruntip, S.; Drouvalakis, K. A.; Kam, N. W. S.; Shim, M.; Li, Y. M.; Kim, W.; Utz, P. J.; Dai, H. J. *Proc. Natl. Acad. Sci. U.S.A.* **2003**, *100*, 4984.
- (12) Besteman, K.; Lee, J.; Wiertz, F. G. M.; Heering, H. A.; Dekker, C. *Nano Lett.* **2003**, *3*, 727.
- (13) Li, C.; Curreli, M.; Lin, H.; Lei, B.; Ishikawa, F. N.; Datar, R.; Cote, R. J.; Thompson, M. E.; Zhou, C. W. *J. Am. Chem. Soc.* **2005**, *127*, 12484.
- (14) So, H. M.; Won, K.; Kim, Y. H.; Kim, B. K.; Ryu, B. H.; Na, P. S.; Kim, H.; Lee, J. O. *J. Am. Chem. Soc.* **2005**, *127*, 11906.
- (15) Patolsky, F.; Zheng, G. F.; Hayden, O.; Lakadamyali, M.; Zhuang, X. W.; Lieber, C. M. *Proc. Natl. Acad. Sci. U.S.A.* **2004**, *101*, 14017.
- (16) Zheng, G.; Patolsky, F.; Cui, Y.; Wang, W. U.; Lieber, C. M. *Nat. Biotechnol.* **2005**, *23*, 1294.
- (17) Bergveld, P. *Sens. Actuators, B* **2003**, *88*, 1.
- (18) Poghosian, A.; Cherstvy, A.; Ingebrandt, S.; Offenhausser, A.; Schoning, M. J. *Sens. Actuators, B* **2005**, *111*, 470.
- (19) Landheer, D.; Aers, G.; McKinnon, W. R.; Deen, M. J.; Ranuarez, J. C. *J. Appl. Phys.* **2005**, *98*, 044701.
- (20) Pouthas, F.; Gentil, C.; Cote, D.; Zeck, G.; Straub, B.; Bockelmann, U. *Phys. Rev. E* **2004**, *70*, 031906.
- (21) Uslu, F.; Ingebrandt, S.; Mayer, D.; Bocker-Meffert, S.; Odenthal, M.; Offenhausser, A. *Biosens. Bioelectron.* **2004**, *19*, 1723.
- (22) Souteyrand, E.; Cloarec, J. P.; Martin, J. R.; Wilson, C.; Lawrence, I.; Mikkelsen, S.; Lawrence, M. F. *J. Phys. Chem. B* **1997**, *101*, 2980.
- (23) vanHal, R. E. G.; Eijkel, J. C. T.; Bergveld, P. *Adv. Colloid. Interface Sci.* **1996**, *69*, 31.
- (24) Bergveld, P. *Biosens. Bioelectron.* **1991**, *6*, 55.
- (25) Rosenblatt, S.; Yaish, Y.; Park, J.; Gore, J.; Sazonova, V.; McEuen, P. L. *Nano Lett.* **2002**, *2*, 869.
- (26) Zhou, C. W.; Kong, J.; Yenilmez, E.; Dai, H. J. *Science* **2000**, *290*, 1552.
- (27) Kong, J.; Dai, H. J. *J. Phys. Chem. B* **2001**, *105*, 2890.
- (28) Star, A.; Han, T. R.; Gabriel, J. C. P.; Bradley, K.; Gruner, G. *Nano Lett.* **2003**, *3*, 1421.
- (29) Oh, J.; Roh, S.; Yi, W.; Lee, H.; Yoo, J. *J. Vac. Sci. Technol., B* **2004**, *22*, 1416.
- (30) Larrimore, L.; Nad, S.; Zhou, X.; Abruna, H.; McEuen, P. L. *Nano Lett.* **2006**, *6*, 1329.
- (31) Iler, R. K. *The Chemistry of Silica*; John Wiley & Sons: New York, 1979.
- (32) Bolt, G. H. *J. Phys. Chem.* **1957**, *61*, 1166.
- (33) Fu, Q.; Liu, J. *Langmuir* **2005**, *21*, 1162.
- (34) Decher, G. *Science* **1997**, *277*, 1232.
- (35) Cao, H.; Wang, Q.; Wang, D. W.; Dai, H. J. *Small* **2005**, *1*, 138.
- (36) Seidel, R.; Liebau, M.; Duesberg, G. S.; Kreupl, F.; Unger, E.; Graham, A. P.; Hoenlein, W.; Pompe, W. *Nano Lett.* **2003**, *3*, 965.
- (37) Christen, H. M.; Poretzky, A. A.; Cui, H.; Belay, K.; Fleming, P. H.; Geoghegan, D. B.; Lowndes, D. H. *Nano Lett.* **2004**, *4*, 1939.
- (38) Cheung, C. L.; Hafner, J. H.; Odom, T. W.; Kim, K.; Lieber, C. M. *Appl. Phys. Lett.* **2000**, *76*, 3136.
- (39) Hafner, J. H.; Cheung, C. L.; Lieber, C. M. *J. Am. Chem. Soc.* **1999**, *121*, 9750.

- (40) Artyukhin, A. B.; Bakajin, O.; Stroeve, P.; Noy, A. *Langmuir* **2004**, *20*, 1442.
- (41) Ladam, G.; Schaad, P.; Voegel, J. C.; Schaaf, P.; Decher, G.; Cuisinier, F. *Langmuir* **2000**, *16*, 1249.
- (42) Neff, P. A.; Naji, A.; Ecker, C.; Nickel, B.; v. Klitzing, R.; Bausch, A. R. *Macromolecules* **2006**, *39*, 463.
- (43) Caruso, F.; Donath, E.; Mohwald, H. *J. Phys. Chem. B* **1998**, *102*, 2011.
- (44) Caruso, F. *Chem.—Eur. J.* **2000**, *6*, 413.
- (45) Israelachvili, J. *Intermolecular and Surface Forces*, 2nd ed.; Academic Press: San Diego, CA, 1992.
- (46) Cui, Y.; Wei, Q. Q.; Park, H. K.; Lieber, C. M. *Science* **2001**, *293*, 1289.
- (47) Abendroth, R. P. *J. Colloid Interface Sci.* **1970**, *34*, 591.
- (48) Dove, P. M.; Craven, C. M. *Geochim. Cosmochim. Acta* **2005**, *69*, 4963.
- (49) Tadros, T. F.; Lyklema, J. *J. Electroanal. Chem.* **1968**, *17*, 267.
- (50) Durstock, M. F.; Rubner, M. F. *Langmuir* **2001**, *17*, 7865.
- (51) Bradley, K.; Cumings, J.; Star, A.; Gabriel, J. C. P.; Gruner, G. *Nano Lett.* **2003**, *3*, 639.
- (52) Losche, M.; Schmitt, J.; Decher, G.; Bouwman, W. G.; Kjaer, K. *Macromolecules* **1998**, *31*, 8893.
- (53) Wong, J. E.; Rehfeldt, F.; Hanni, P.; Tanaka, M.; Klitzing, R. V. *Macromolecules* **2004**, *37*, 7285.
- (54) Tedeschi, C.; Mohwald, H.; Kirstein, S. *J. Am. Chem. Soc.* **2001**, *123*, 954.

NL061343J